Journal of Theoretical Biology 280 (2011) 34–42

Contents lists available at ScienceDirect

Journal of Theoretical Biology

journal homepage: www.elsevier.com/locate/yjtbi

A model of localised Rac1 activation in endothelial cells due to fluid flow

R.J. Allen [a,*], I.D.L. Bogle [a], A.J. Ridley [b]

[a] Centre for Mathematics and Physics in the Life Sciences and Experimental Biology (CoMPLEX), University College London, Gower Street, London WC1E 7JE, United Kingdom
[b] Randall Division of Cell and Molecular Biophysics, Kings College London, New Hunts House, Guys Campus, London SE1 1UL, United Kingdom

ARTICLE INFO

Article history:
Received 1 June 2010
Received in revised form
7 March 2011
Accepted 17 March 2011
Available online 23 March 2011

Keywords:
Stokes flow
Endothelial cell
Rho GTPases
Src
Shear stress

ABSTRACT

Endothelial cells respond to fluid flow by elongating in the direction of flow. Cytoskeletal changes and activation of signalling molecules have been extensively studied in this response, including: activation of receptors by mechano-transduction, actin filament alignment in the direction of flow, changes to cell-substratum adhesions, actin-driven lamellipodium extension, and localised activation of Rho GTPases. To study this process we model the force over a single cell and couple this to a model of the Rho GTPases, Rac and Rho, via a Kelvin-body model of mechano-transduction. It is demonstrated that a mechano-transducer can respond to the normal component of the force is likely to be a necessary component of the signalling network in order to establish polarity. Furthermore, the rate-limiting step of Rac1 activation is predicted to be conversion of Rac-GDP to Rac-GTP, rather than activation of upstream components. Modelling illustrates that the aligned endothelial cell morphology could attenuate the signalling network.

1. Introduction

Endothelial cells (ECs) respond to fluid flow by elongating in the direction of flow (Davies, 1995; Ballerman et al., 1998; Wojciak-Stothard and Ridley, 2003; Tzima et al., 2002; McCue et al., 2006). This response is believed to be crucial for the correct function of the endothelium. Atherosclerotic plaques usually localize in regions of turbulent blood flow (for example, at sites of arterial branching). In these regions the endothelium has increased permeability and ECs take on a rounded morphology. This is in contrast to their ellipsoidal shape in regions of smooth flow (Weinbaum et al., 1985; Ross, 1999). Hence, there is a correlation (although not necessarily causation) between EC morphology and atherosclerotic plaques.

In order to respond to fluid flow, ECs must be able to transduce the mechanical force of the fluid into a biochemical signal. This mechano-transduction is likely to be mediated by activation of proteins via conformational changes due to increased tension or compression. A number of different proteins have been implicated in mechano-transduction, including cell–cell adhesion proteins such as PECAM-1 (Chiu et al., 2008; Tzima et al., 2005), stretch-activated ion channels (Martinac, 2004), and integrin-associated proteins in focal adhesions (FAs). Integrins are transmembrane hetero-dimers that anchor the cell to the extracellular matrix (ECM). Hence if the cell is to remain adherent they must experience an increase in tensile force following the onset of fluid flow. This force is transmitted through the cytoskeleton to FAs. Integrins have been shown to respond to fluid flow (Tzima et al., 2001) and to be locally activated at the downstream edge (Goldfinger et al., 2008). However, this may be due to increased integrin–ECM ligation. The role of FAs and integrins is further supported by early FA remodelling (Davies et al., 1994) and fast activation of the integrin-associated tyrosine kinase Src (Wang et al., 2005a). p130Cas, an adaptor protein, is a known mechano-transducer associated with FAs, and can be activated in response to mechanical stretching (Sawada et al., 2006). It is also activated through Src-induced tyrosine phosphorylation (Okud et al., 1999).

Mechano-transduction and cellular mechanics have been extensively modelled previously (Mazzag et al., 2003; Stamenovic et al., 1996; Schwarz et al., 2005; Herant et al., 2003). For example, force transduction through ECs has been modelled using Kelvin bodies in parallel and in series (Mazzag et al., 2003) and focal adhesions have been modelled using a two spring model (Schwarz et al., 2005). Cell structure has been described by a tension-integrity model, and has been applied to a discrete system of struts (microtubules) and cables (actin filaments) (Stamenovic et al., 1996). This model demonstrated that stiffness of the model cell increased with pre-stress generated by actin–myosin contraction. Aspects of neutrophil mechanics have been successfully described using a two-phase model of reactive interpenetrating flows (Herant et al., 2003).

The Rho GTPases Rho and Rac regulate both FA formation and endothelial shape changes in response to fluid flow. Rho GTPases regulate cytoskeletal dynamics and contribute to many cellular

* Corresponding author. Present Address: Department of Pharmacology, University of North Carolina, Chapel Hill, North Carolina 27599, USA.
E-mail address: richard.allen@unc.edu (R.J. Allen).

0022-5193/$ - see front matter © 2011 Elsevier Ltd. All rights reserved.
doi:10.1016/j.jtbi.2011.03.021

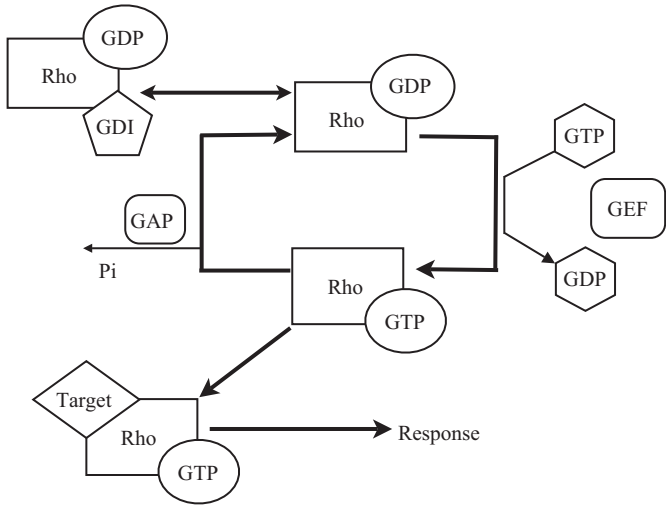

Fig. 1. Rho GTPase regulation by GAPs, GEFs and GDIs. In the inactive state (GDP bound) the GTPase interaction with the plasma membrane is inhibited by interaction with a GDI, which in turn prevents activation. The GEF removes GDP from the GTPase. Subsequent binding of GTP occurs quickly (because of the high ratio of GTP to GDP). The rate of hydrolysis of RhoGTP is increased by binding of a GAP (DerMardirossian and Bokoch, 2005; Bos et al., 2007).

responses including cell migration and cytokinesis (Ridley, 2001; Narumiya and Yasuda, 2006; Ridley, 2006; Jaffe and Hall, 2005). Rho GTPases switch between an inactive guanosine diphosphate (GDP) bound form and an active guanosine triphosphate (GTP) bound form which interacts with downstream effectors. Switching between these two forms usually occurs on the membrane and is regulated by guanine nucleotide exchange factors (GEFs), GTPase-activating proteins (GAPs) and guanine dissociation inhibitors (GDIs; see Fig. 1).

RhoA leads to acto-myosin contraction via Rho kinases (ROCKs) and myosin light chain (MLC) phosphorylation (Riento and Ridley, 2003; Kawano et al., 1999). In response to fluid flow, RhoA has been reported to contribute to cell shape change by transiently inducing cell contraction, subsequently allowing cells to elongate in the direction of flow (Wojciak-Stothard and Ridley, 2003). Rac activation is localised to the downstream edge in ECs responding to fluid flow (Tzima et al., 2002). In response to integrin activation, Src has been shown to activate a Rac GEF, Vav2 (Garrett et al., 2007), and p190RhoGAP (a GAP for Rho) (Arthur et al., 2000). Thus, in this context, activation of Rac and inhibition of Rho is hypothesised to occur. In addition, it is believed that inhibitory crosstalk between Rho and Rac leads to separate zones of activation (Jilkine et al., 2007; Narang, 2006).

In order to investigate how the interplay between mechanical forces and EC morphology can influence downstream signalling, the work presented here models the mechanical force, transduction of the mechanical force into a biochemical signal and the downstream signalling to Rac1. We will describe three coupled computational models of these processes: fluid flow over an EC attached to a planar surface, mechano-transduction on the basal surface and signalling to Rac1. The flow model predicts the force on the surface of the cell. This force is coupled to a biochemical model via a mechano-transduction model.

2. The flow model

To establish a possible mechanism linking the force on an EC to localised Rac activation, the fluid flow, $\mathbf{u}$, is modelled over a single cell attached to a planar surface ($z=0$) by the Stokes equation:

$$-\nabla P+\mu\nabla^2\mathbf{u}+\rho\mathbf{b}=0 \tag{1}$$

where P is the pressure and μ and ρ are the viscosity and density of the fluid respectively. On the characteristic length and time scales of this problem the Reynolds number is very small. Thus, assuming Newtonian characteristics, the fluid is well modelled by Eq. (1). Here the Stokes equation is solved by using a boundary integral representation, which has previously been used in this context (Hazel and Pedley, 2000; Wang and Dimitrakopoulos, 2006a,b). In this representation the fluid flow at $u_j(\mathbf{x}_0)$ is given by:

$$u_j(\mathbf{x}_0)=u_j^{\infty}(\mathbf{x}_0)-\frac{1}{8\pi\mu}\int_S f_i(\mathbf{x}_0)G_{ij}(\mathbf{x},\mathbf{x}_0)\,dS \tag{2}$$

where $\mathbf{u}^{\infty}(\mathbf{x}_0)=(kz,0,0)$ is the flow far away from the cell, S is the cell surface, f_i is the surface force and G_{ij} is a Green's function that vanishes if $\mathbf{x}\in S$ (Pozrikidis, 1992; Blake, 1971; Higdon, 1985). Intuitively Eq. (2) represents a sum of point forces weighted so that the boundary conditions are satisfied. It is these weights that are the unknowns.

To solve for the unknowns the cell surface is discretised into n triangles (Fig. 2). The surface is defined by:

$$z=\begin{cases} H\dfrac{(R^2-r^2)}{R^2} & \text{when } r^2<R^2 \\ 0 & \text{otherwise} \end{cases} \tag{3}$$

where H is the maximum height of the EC, $R=20$ μ is the typical radius of an approximately circular (in the $x-y$ plane) EC and $r^2=ax^2+b^2$. Unless otherwise noted, $a=b=1$, Fig. 2. It is supposed that the EC is not adapted to flow, and the height of the EC is taken to be $H=6$ μm. Depending on conditions, and EC type, ECs vary in height from 1 to 12 μm (Wee et al., 2009; Barbee et al., 1994).

To facilitate the solution of a system of partial differential equations (to model reaction–diffusion), the discretization is chosen such that the projection of the surface nodes onto the plane $z=0$ gives a hexagonal lattice, with each hexagon composed of four of the surface element triangles. In the following results the area of the hexagons is 1.66 μm^2, corresponding to a side length of 0.8 μm. Eq. (2) is solved by applying the no-slip boundary condition on S; $\mathbf{u}(\mathbf{x}_0)=0$ if $\mathbf{x}_0\in S$. A linear problem for the unknown surface force can be formed by applying the discrete version of Eq. (2) at n points on S, $\mathbf{x}_0$. The surface force is assumed constant over surface elements. The linear problem for the $f_i(\mathbf{x}_0)$ is solved by an iterative Krylov subspace method (Saad, 1981). The numerical method was validated on a hemisphere surface (in contrast to the surface described by Eq. (3)) and compared to a known approximate analytical solution for the non-dimensional total force on this surface due to shear flow ($F=4.30\pi$, (Price, 1985)) and was

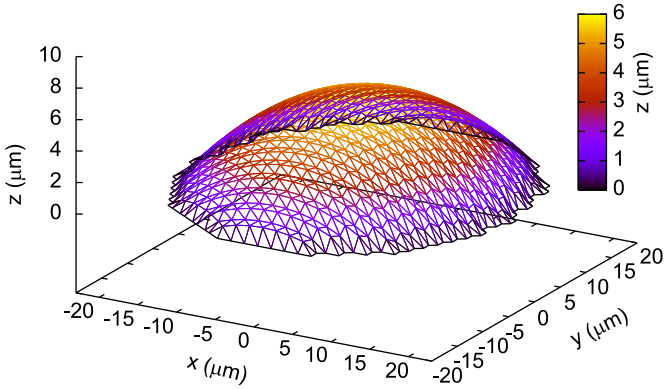

Fig. 2. An individual cell's (attached to a plane at $z=0$) surface discretised into a triangle mesh, such that the projection on the $x-y$ plane of the mesh nodes gives the vertices of hexagons. The fluid flow is in the positive x direction: $\mathbf{u}=(kz,0,0)$, $z\geq 0$.

Table 1
Model parameters. See references for accuracy in parameter values. Parameters estimated in the appendix are determined up to an order of magnitude.

Parameter	Description	Value	Units	Source
D_m	Membrane diffusion	0.1	$\mu m^2\ s^{-1}$	Marèe et al. (2006)
D_{mc}	Membrane and cytosol diffusion	10	$\mu m^2\ s^{-1}$	Marèe et al. (2006)
k	Shear rate	280	s^{-1}	See Appendix
μ	Fluid viscosity	1×10^{-6}	$g\ \mu m^{-1}\ s^{-1}$	See Appendix
v	Dashpot viscosity	6.33×10^{-5}	Pa m s	Mazzag et al. (2003)
h_1	Spring constant	1.25×10^{-3}	Pa m	Mazzag et al. (2003)
h_2	Spring constant	1.61×10^{-3}	Pa m	Mazzag et al. (2003)
$k_+(z_e)$	Extension dependent Src activation	Fig. 8	s^{-1}	See Appendix
k_-	Src inactivation rate	0.006	s^{-1}	See Appendix
k_1	GEF activation	0.83	$\mu M^{-1}\ s^{-1}$	See Appendix
k_2	GEF inactivation	0	$\mu M^{-1}\ s^{-1}$	See Appendix
k_3	Rac GEF binding rate	0.0034	$\mu M^{-1}\ s^{-1}$	Zhang et al. (2000)
k_4	Rac GEF unbinding rate	1.1×10^{-6}	s^{-1}	Zhang et al. (2000)
k_5	Rac GDP disassociation	0.094	s^{-1}	Zhang et al. (2000)
k_6	Rac GAP binding	0.017	$\mu M^{-1}\ s^{-1}$	Goryachev and Pokhilko (2006)
k_7	Rac GAP unbinding	0.05	s^{-1}	Goryachev and Pokhilko (2006)
k_8	RacGTP GAP hydrolysis	8.3	s^{-1}	Goryachev and Pokhilko (2006)
k_9	Rac GAP activation	0.001	$\mu M^{-1}\ s^{-1}$	See Appendix
k_{10}	Rac GAP inactivation	0	$\mu M^{-1}\ s^{-1}$	See Appendix
k_{11}	Rho GAP activation	0.8	$\mu M^{-1}\ s^{-1}$	See Appendix
k_{12}	Rho GAP inactivation	0	$\mu M^{-1}\ s^{-1}$	See Appendix
k_{13}	Rho GAP binding	0.017	$\mu M^{-1}\ s^{-1}$	$=k_6$
k_{14}	Rho GAP unbinding	0.05	μs^{-1}	$=k_7$
k_{15}	RhoGTP GAP hydrolysis	8.3	μs^{-1}	$=k_8$
k_{16}	Rho GEF binding rate	0.0034	$\mu M^{-1}\ s^{-1}$	$=k_3$
k_{17}	Rho GEF unbinding rate	1.1×10^{-6}	s^{-1}	$=k_4$
k_{18}	Rho GDP disassociation rate	0.094	s^{-1}	$=k_5$
k_{19}	Rho GEF activation	0	$\mu M^{-1}\ s^{-1}$	See Appendix
k_{20}	Rho GEF inactivation	0.0001	$\mu M^{-1}\ s^{-1}$	See Appendix
k_{21}	basal Rho GAP activation	0.002	s^{-1}	See Appendix
k_{22}	basal Rho GAP inactivation	0.009	s^{-1}	See Appendix
k_{23}	basal Rac GEF activation	0.00045	s^{-1}	See Appendix
k_{24}	basal Rac GEF inactivation	0.09	s^{-1}	See Appendix
k_{25}	basal Rac GAP activation	0.002	s^{-1}	See Appendix
k_{26}	basal Rac GAP inactivation	0.004	s^{-1}	See Appendix
k_{27}	basal Rho GEF activation	0.00045	s^{-1}	See Appendix
k_{28}	basal Rho GEF inactivation	0.015	s^{-1}	See Appendix

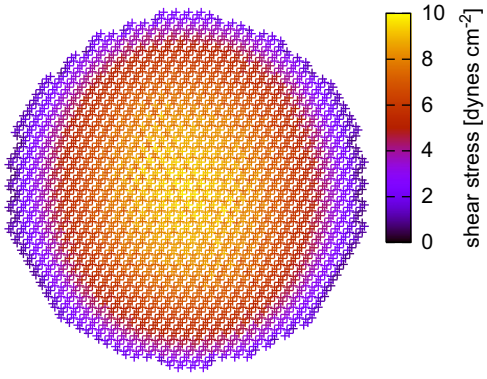

Fig. 3. Shear stress on the cell in Fig. 2 (projected on the plane $z=0$) and subjected to laminar fluid flow (left to right). Note that the shear is symmetrical with respect to the upstream and downstream edges.

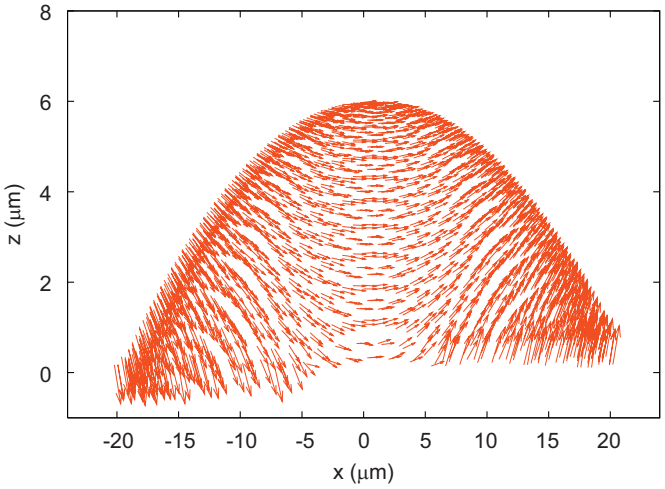

Fig. 4. Unit force, $\hat{f}$, on the surface of the cell (as in Figs. 2 and 3) due to laminar fluid flow (left to right). Note that the upstream edge of the cell is in compression and the downstream edge is under tension.

found to be accurate up to an error of 1.7% for 3000 surface elements.

2.1. Results

All parameters are given in Table 1. Fig. 3 gives the pattern of shear stress on the cell surface as a result of flow in a large artery. Under these conditions the maximum shear stress is 10 dyn cm^{-2}, which is similar to the wall shear stress calculated in *in vitro* flow chamber experiments (Wojciak-Stothard and Ridley, 2003; Tzima et al., 2001, 2002).

It is evident that the force component normal to the surface of the cell could give rise to the spatial heterogeneity via separate regions of tension and compression (Fig. 4). For a symmetric cell,

the tangential surface component is symmetrical with respect to the upstream and downstream points of the cell (Fig. 3). Although the surface component could be crucial for signalling via ion channels, this signalling would (assuming uniform distributions of channels) initially lead to global changes in the cell.

3. Force transduction and GTPase signalling

The force on the cell surface is coupled to the network (Fig. 7), which is modelled below, by treating integrins as a Kelvin body, Fig. 5. Previously, Ferko et al. (2007) showed that heterogeneity in intra-cellular structure could play an important role in the sub-cellular localization of mechano-transduction. However, here we make the simplifying assumptions that the cytosol/cytoskeletal medium is uniform and that force is transmitted to the basal surface locally. Both shear and normal forces are borne by cytoskeletal elements and, potentially, could activate mechano-transducers either at the basal surface or at ion channels in the membrane. However, the hypothesis we aim to test is whether a response to the force normal to the surface could be responsible for breaking the symmetry in the upstream and downstream signalling regions. Hence, to test whether the magnitude of the normal force could stretch a mechano-transducer by a biologically relevant amount we coupled the Kelvin body model, Fig. 5, to the force due to fluid flow.

The equation governing the Kelvin body (Mazzag et al., 2003), given that the force is constant, is

$$v\left(1+\frac{h_1}{h_2}\right)\frac{dz_e}{dt}=h_1 z_e - F \tag{4}$$

where F is the force on the body and z_e is its extension. Only tensile forces are considered and, to simplify the model, a smooth concentration of integrins is assumed; that is, clustering is ignored. Interestingly, Ferko et al. (2007) illustrated that focal adhesions focus and amplify shear forces on the apical surfaces of ECs. Hence, the coarse grained approach applied here provides a conservative estimate for the force applied at the basal surface. The parameters for modelling integrins as a Kelvin body have been fitted to experimental data (Bausch et al., 1999). The normal force on the cell surface is of the order of pN, leading to an extension of the mechano-transducer in the order of nanometres, Fig. 6.

This model is coupled to a model of Rho GTPase interaction, Fig. 7, by up-regulation of Src activation, Fig. 8. The coupling, between extension (z_e) and the biochemical network (Fig. 7) is via the parameter $k_+(z_e)$, which—in the model—is the rate of Src activation. Src has been shown to be activated (either directly or indirectly) by both shear stress and applied mechanical force (Wang et al., 2005b; Jalali et al., 1998; Fleming et al., 2005). Furthermore, there is evidence that stretch activation exhibits behaviour similar to Fig. 8. For example, in response to mechanical stretching PECAM-1 has switch like, saturating, activation (Chiu et al., 2008). However, for quantitative parameter estimation for the Src activation coupling (Fig. 8) it was necessary to use a course fitting to other experimental data, see Appendix.

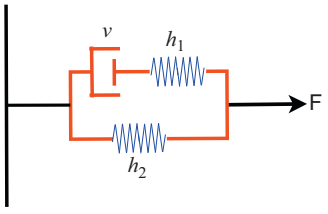

Fig. 5. Kelvin body model of integrin deformation under a force F, with spring constants h_1 and h_2 and dash-pot viscosity μ.

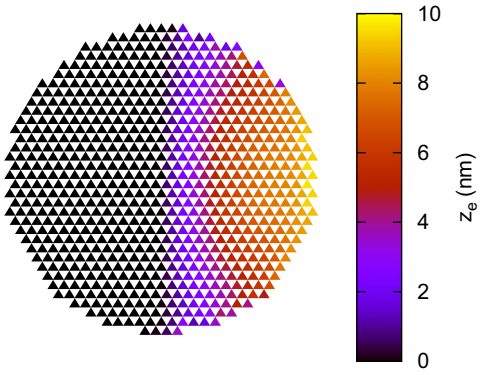

Fig. 6. The force normal to the cell surface is applied to the Kelvin body, Fig. 5, to give a predicted pattern of integrin deformation. Note that compressive forces were assumed not to affect mechano-transducter signalling and, for simplicity, integrin clustering was coarse-grained into a smooth distribution.

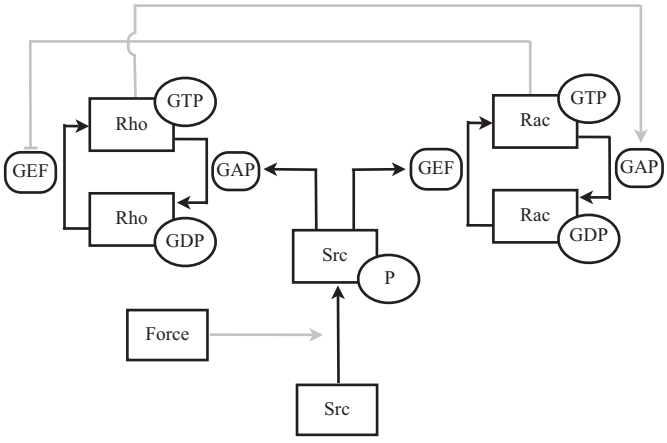

Fig. 7. Rho, Rac and Src network. Force on the cell leads (indirectly) to Src tyrosine phosphorylation. Phosphorylated Src can activate a Rho GAP as well as a Rac GEF, leading to Rac activation and Rho inhibition. Rho and Rac mutually inhibit each other, RhoGTP by activating a Rac GAP and RacGTP inhibits Rho by inhibiting a Rho GEF.

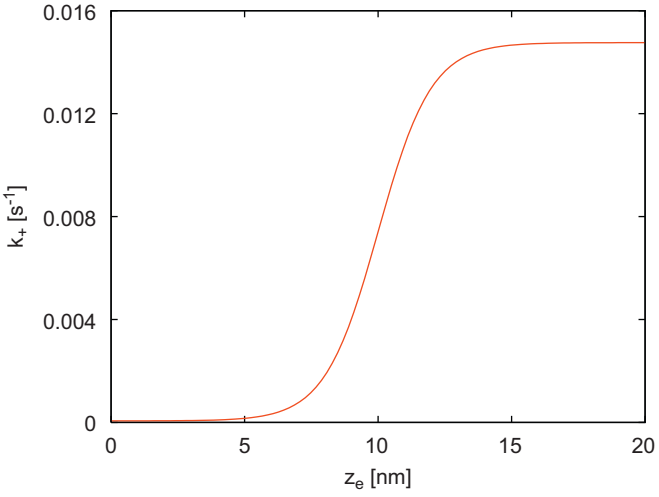

Fig. 8. Up-regulation of the forward Src activation rate $k_+(z_e)$, Eq. (5), as a function of mechano-transducer extension z_e: $k_+(z_e)=0.0006+0.0147/\ (1+e^{(k_e-z_e)})$, where $k_e=10$ nm.

In the model, the resulting Src activation activates the Rho GTPase Rac1. Rho GTPases have previously been modelled in a variety of contexts (Jilkine et al., 2007; Goryachev and Pokhilko, 2006; Sakumura et al., 2005; Marée et al., 2006).

Civelekoglu-Scholey et al. (2005) modelled GTPase activation in this context, but with broader scope and less details of the activation of Rho GTPases themselves.

There is no feedback in this system so once activated there is no return to basal values. The reactions governing the network in Fig. 7 are

$$\mathrm{Src}\ \underset{k_-}{\rightleftharpoons}^{k_+(z_e)}\ \mathrm{Src}^*$$

$$\mathrm{Src}^* + \mathrm{GEF}_R\ \underset{k_2}{\rightleftharpoons}^{k_1}\ \mathrm{Src}^* + \mathrm{GEF}_R^*$$

$$\mathrm{RacGDP} + \mathrm{GEF}_R^*\ \underset{k_4}{\rightleftharpoons}^{k_3}\ \mathrm{RacGDP}-\mathrm{GEF}_R^*\ \overset{k_5}{\rightarrow}\ \mathrm{Rac} + \mathrm{GEF}_R^*$$

$$\mathrm{RacGTP} + \mathrm{GAP}_R^*\ \underset{k_7}{\rightleftharpoons}^{k_6}\ \mathrm{RacGTP}-\mathrm{GAP}_R^*\ \overset{k_8}{\rightarrow}\ \mathrm{RacGDP} + \mathrm{GAP}_R^*$$

$$\mathrm{RhoGTP} + \mathrm{GAP}_R\ \underset{k_{10}}{\rightleftharpoons}^{k_9}\ \mathrm{RhoGTP} + \mathrm{GAP}_R^*$$

$$\mathrm{Src}^* + \mathrm{GAP}_\rho\ \underset{k_{12}}{\rightleftharpoons}^{k_{11}}\ \mathrm{Src}^* + \mathrm{GAP}_\rho^*$$

$$\mathrm{RhoGTP} + \mathrm{GAP}_\rho^*\ \underset{k_{14}}{\rightleftharpoons}^{k_{13}}\ \mathrm{RhoGTP}-\mathrm{GAP}_\rho^*\ \overset{k_{15}}{\rightarrow}\ \mathrm{RhoGDP} + \mathrm{GAP}_\rho^*$$

$$\mathrm{RhoGDP} + \mathrm{GEF}_\rho^*\ \underset{k_{17}}{\rightleftharpoons}^{k_{16}}\ \mathrm{RhoGDP}-\mathrm{GEF}_\rho^*\ \overset{k_{18}}{\rightarrow}\ \mathrm{Rho} + \mathrm{GEF}_\rho^*$$

$$\mathrm{RacGTP} + \mathrm{GEF}_\rho^*\ \underset{k_{20}}{\rightleftharpoons}^{k_{19}}\ \mathrm{RacGTP} + \mathrm{GEF}_\rho$$

$$\mathrm{GAP}_\rho\ \underset{k_{22}}{\rightleftharpoons}^{k_{21}}\ \mathrm{GAP}_\rho^*$$

$$\mathrm{GEF}_R\ \underset{k_{24}}{\rightleftharpoons}^{k_{23}}\ \mathrm{GEF}_R^*$$

$$\mathrm{GAP}_R\ \underset{k_{26}}{\rightleftharpoons}^{k_{25}}\ \mathrm{GAP}_R^*$$

$$\mathrm{GEF}_\rho\ \underset{k_{28}}{\rightleftharpoons}^{k_{27}}\ \mathrm{GEF}_\rho^* \qquad (5)$$

where the subscript R refers to Rac and ρ to Rho. For example GAP_ρ is a GAP for Rho. Active forms are denoted by an asterisk. The nucleotide free GTPases are assumed to quickly bind to GTP (due to the high intracellular GTP:GDP ratio).

Reactions (5) are modelled mathematically as second-order mass action reaction diffusion equations. For example, for a complex A_j interacting with complexes A_i $0 \le i \le n$ the time evolution of the concentration of A_i at time t and position $\mathbf{x}$, $A_i(\mathbf{x},t)$, is modelled as

$$\frac{\partial A_i}{\partial t} = \sum_{j=0}^{n} \alpha_j A_j + \sum_{k=0}^{n}\sum_{j=0}^{n} \beta_{jk} A_j A_k + D_i \nabla^2 A_i$$

Applying this equation to reactions (5) gives a partial differential equation for each species in Fig. 7 with α_j and β_{jk}. Clearly most of the α_j and β_{jk} are zero since most species do not interact in this scheme (Fig. 7)—the non-zero values correspond to the reaction rates (k_1–k_{28}).

As a generalisation only two values are taken for D_i, corresponding to whether A_i is solely membrane bound (GEFs, RacGTP, RhoGTP, Src), or membrane and cytosol bound. Here the GDIs are not modelled explicitly. Jilkine et al. (2007) proposed a quasi-steady state between GDI bound and unbound GTPases. The effect of this is a modified diffusion coefficient to take into account the diffusion on the membrane and in the cytosol for the GDP bound GTPase. This is the approach followed here. It is also assumed that the GAPs and GEFs are specific for either Rho or Rac but not both (Rossman et al., 2005; Tcherkezian and Lamarche-Vane, 2007); in reality this need not be the case. The effect of this additional level of coupling is a direction of future research.

The PDEs were integrated on a 2-D projection of the cell surface mesh. This projection was designed so that the projected mesh defined a hexagonal grid. The PDEs were integrated on this grid by a simple Euler method with the spatial derivative approximated by central differences. On the time-scale of interest it was assumed that the cell was impermeable. Hence, no flux boundary conditions were implemented using reflective conditions at the cell edge.

It was assumed that the transmission of the force on the cell due to fluid flow is fast relative to Src activation. Hence, the mechano-transducer extension (Fig. 6) is taken to occur instantaneously. This extension (predicted by the flow model coupled with the mechano-transduction model) leads to Src activation and is the input signal to the reaction network, Fig. 7.

3.1. Results

Applying these equations on the cell (which is now a 2-D projection) gives localised Src and Rac activation in the downstream edge, Fig. 9. Using the derived parameters (see Appendix) the time-course of Src activation is comparable to previously reported (Fleming et al., 2005; Jalali et al., 1998). The whole cell response for Rac, Fig. 9(d), is slightly less than reported (Tzima et al., 2002). However, the model predicts maximal Rac activation within 25 min, which is comparable to the observed response (Tzima et al., 2002). Interestingly, the rates of GEF_R activation due to active Src reach new steady states relatively quickly, and it is actually the rates of GAP and GEF catalysed GDP-GTP exchange which are the rate limiting ones. The pattern of Rac activation, Fig. 9(b), is generated by localised Src activation; however it is maintained due to mutual Rho and Rac inhibition (though with removal of this cross-talk a similar, albeit less distinct, pattern as shown in Fig. 9(b) occurs — not shown) and slow diffusion of the active membrane bound RacGTP. It is also crucial that the RacGDP–GEF intermediary is membrane bound. Fig. 10 shows the same equations solved whilst taking this intermediary as diffusing both on the membrane and in the cytosol. With this higher diffusion rate, even of this relatively short-lived intermediary, the Rac activation pattern is destroyed, Fig. 10(a), whereas the whole cell measure of Rac activation, Fig. 10(b), is broadly similar to Fig. 9(d). Whole cell profiles of activation therefore characterise the system poorly, and thus to test and generate hypotheses of EC responses to fluid flow it is necessary to have experimental data that quantifies local activation of proteins.

Previous experimental work has shown activation of Rac and inhibition of Rho returning to basal levels after an extended period of time (Tzima et al., 2001, 2002; Wojciak-Stothard and Ridley, 2003). In this current model there is no feedback, so the new steady states are maintained. However it is not necessarily the case that there must be direct biochemical feedback. It is possible that the change in morphology itself is enough to damp the system back to basal levels, i.e. as the cell polarizes the signal from the flow is attenuated. After long term exposure to shear stress ECs flatten to approximately 50% of their original height, which reduces the total and maximum shear on their surface (Barbee et al., 1994). This could switch off the signalling network. However a cell elongated (and flattened) in one direction would not align with the flow in a different direction if this was the only effect. The EC orientation may play an important role in modulating the signal. Cells orientated perpendicular ($a=1/3$ and $b=3$, Eq. (3)) to the flow have a higher response (as measured by Rac-GTP) than parallel ($a=3$ and $b=1/3$, Eq. (3)) and symmetric cells (Fig. 11). This effect may be amplified by clustering of integrins: if they are localised in FA then the location of FAs with respect to the up and downstream regions of the cell could be important.

Fig. 11(d) shows Rho inhibition across the whole cell: the concentration distribution of Rho-GTP is more homogenous (not shown) than the Rac-GTP distribution because Src activates GAP_ρ which can diffuse relatively quickly through the cell. Some experiments report rapid transient activation of Rho (Wojciak-Stothard and Ridley, 2003), but this could be through a different pathway (either via integrins or a different mechano-transduction mechanism).

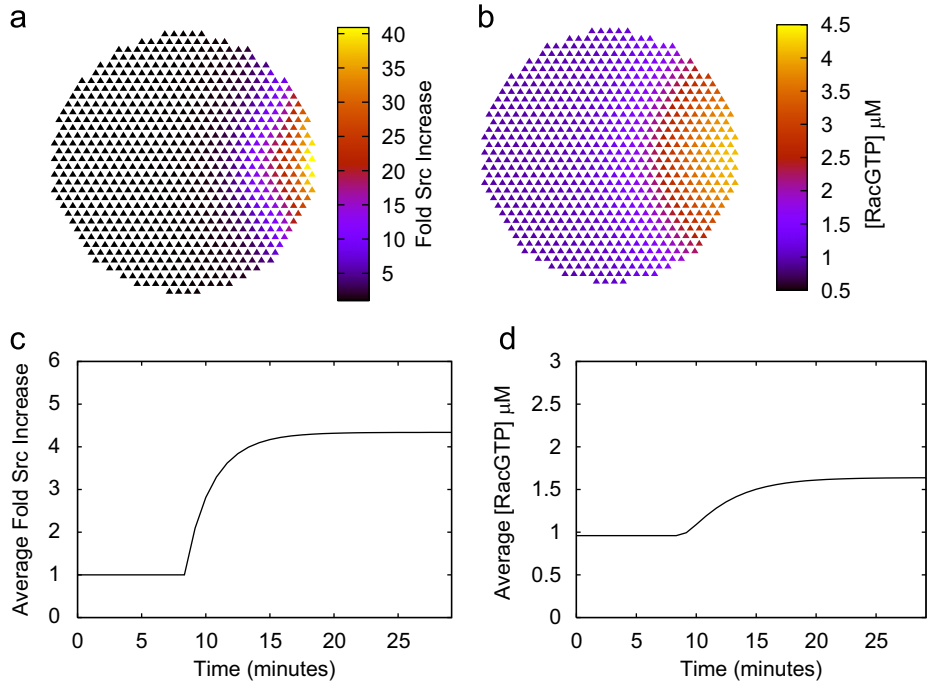

Fig. 9. Src and Rac activation due to fluid flow (left to right) as generated by the model equations (5). (a) Src activation on a 2-D projection of the cell (Fig. 2) according to the Kelvin body model coupled to reaction (5) via Fig. 8. (b) Subsequent RacGTP concentration distribution in the cell. (c) Fold Src increase over the whole cell. This is fixed by parameter estimation (Appendix) to give a similar response as found experimentally (Fleming et al., 2005; Jalali et al., 1998). (d) Average RacGTP concentration over the whole cell.

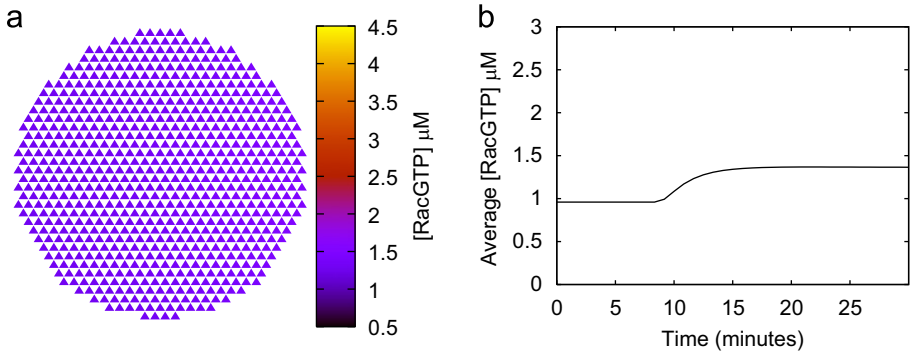

Fig. 10. The effect of allowing the RacGDP-GEF intermediary (Eqs. (5)) to diffuse in the cytosol and on the membrane as oppose to just on the membrane as in Fig. 9(b). A localised pattern of activation is not generated, though the average [RacGTP] is similar as in 9(d). (a) Concentration distribution of RacGTP. (b) Average RacGTP concentration over the whole cell.

4. Discussion

Exactly how ECs interpret the force due to fluid flow and how the components of the process interact remain an open question. Here, coupling models of fluid flow, mechano-transduction and Rho GTPase activation we have tested a plausible mechanism of interpreting the flow by a mechano-transducer and downstream signalling (the Rho GTPases RhoA and Rac1). The strength of this work is the coupling of the multi-scale models from fluid flow through localized biochemical signalling.

The hypothesis presented here is that there is a mechano-transducer that is sensitive to the force normal to surface. We suggest that this mechano-transducer is activated in a region localized near the applied force, and tested whether this could lead to spatial localization of Rac1 activity (i.e. given the pattern of normal force and diffusion of some key components of the signalling network, can local activation of Rac1 be initiated). If our hypothesis had failed using this model then we would also expect it to fail on inclusion of a more complete consideration of cytoskeletal biomechanics and shear force.

The mechano-transduction model is a simplified first approximation and only one component of the force was considered. This model could be developed to allow force in any direction. However, to do so would require a more sophisticated treatment of cytoskeletal mechanics—which was beyond the scope of this work. This would be a particularly interesting future direction; the heterogeneity and complexity of cellular structure may lead to unexpected conclusions regarding the transmission of force through ECs. For example, more realistic models of large focal adhesions in discrete locations, rather than the coarse grained continuous adhesions assumed here, could potentially lead to distinct conclusions.

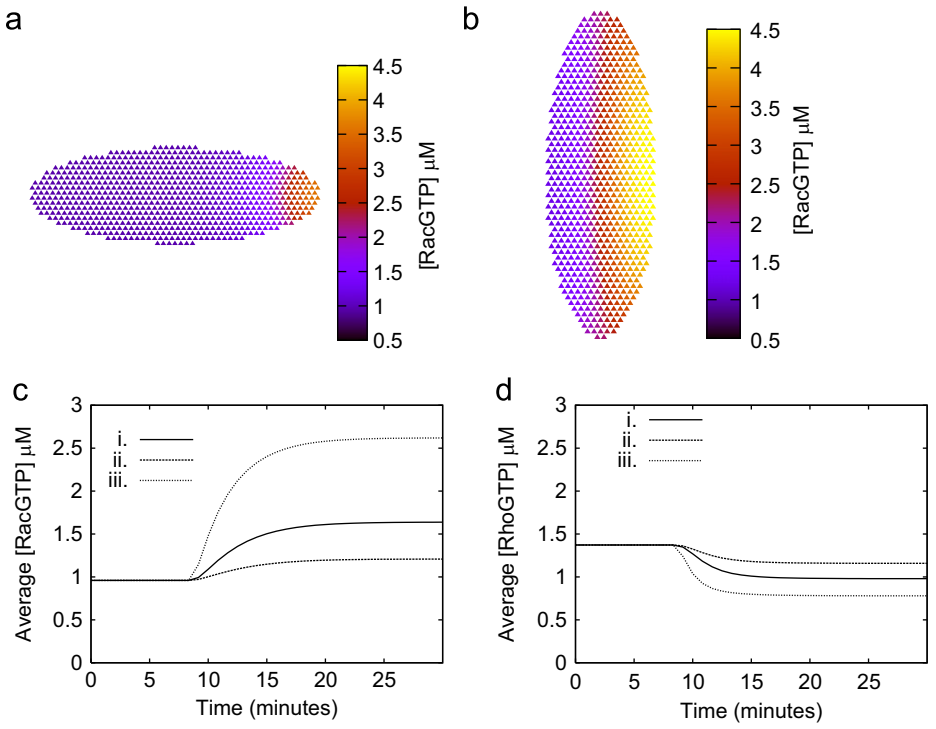

Fig. 11. Rac activation due to fluid flow (left to right in (a) and (b)) as generated by the reactions (5) for different cell morphologies with the same volume and maximum height as Fig. 9(b). (a) RacGTP concentration for a cell already aligned with the flow. (b) RacGTP concentration distribution for a cell aligned perpendicular to the flow. (c) and (d) Mean RacGTP and RhoGTP concentrations (respectively) over the whole cells: (i) cell shape as in 9(b), (ii) Fig. 11(a), (iii) Fig. 11(b).

This work implies that the heterogeneity of the force normal to the cell surface could give rise to the polarized signalling response. It has previously been suggested that the normal force could play an important role in EC signalling (Wang and Dimitrakopoulos, 2006a,b)). Response to the normal force may be a necessary component of the process of EC polarization and alignment, although it is probably not sufficient. It is probable that mechano-transduction via other pathways could supplement the model here. For example, it is possible that the ion channels could either respond to the normal component of the force in some manner, perhaps due to cytoskeleton coupling (Barakat et al., 2006), or are pre-oriented asymmetrically. Precisely how ECs transduce and respond to a mechanical force are unclear. However, modelling has also shown if cells respond to the normal force then a change in the morphology of the cell itself may attenuate signalling. In particular, the orientation of cells with respect to the cell can, potentially, lead to very different signalling. This suggests a plausible mechanism for cells sensing the direction of the flow and whether, given their current morphology, they should respond to the flow.

Here, a plausible mechanism for signal transduction is presented. Src is taken as a read-out of FA signalling, but it should be noted that it is likely that there are many intermediaries linking FA signalling and Rho GTPase activity. Hence, further work is required to establish, either computationally or experimentally, the complete nature of FA signalling in response to fluid flow. Components of integrin complexes are known to respond to force. However, the exact nature of the mechano-transduction is unclear.

Src, a tyrosine kinase associated with integrins, was taken as a biochemical measure of EC response to force and hypothesised to link directly to Rac GEF and Rho GAP activation. This hypothesis was tested with a simple model of Rho GTPase cross-talk and cycling (between GTP- and GDP-bound forms). Modelling showed that this hypothesis could lead to GTPase activation comparable to the reported levels for whole cell averages and qualitatively similar to localized regions of Rac activation.

It is evident that the Rho GTPases make excellent candidates for triggering local cytoskeleton events. Acting as switches they can be highly regulated by GEFs and GAPs and, furthermore, their association with the plasma membrane (once activated) means that the activation is kept in locally distinct areas due to slow diffusion. Thus to generate localised patterns of Rho GTPase activation, it seems that either a bistability is established or that it is the GEF that is activated rather than a GAP inactivated. In the latter case the faster diffusing GAP will result in activation being a more global phenomenon, similar to Fig. 10. The mechanism presented here is similar to a more general suggestion for local activation of GTPases (Bement et al., 2006). It is also demonstrated that measures of activation across the whole cell cannot distinguish between different hypotheses; more local measures of protein activity in response to fluid flow are required to make such a determination.

In principle this hypothesis could be valid in an alternative form with a different read out from integrin complex signalling and a different link between GEFs and GAPs and the mechano-transducer. However, it does seem clear that the normal component of the force on the EC must play a role in initiating the heterogeneity in signalling, however the model here could be augmented by different pathways resulting from either integrin, ion channel or cell junction mechano-transduction.

Appendix A

See the table below for the parameters used in this work.

A.1. Flow parameters

The shear rate is estimated by modelling the flow for a steady Newtonian fluid in a large cylinder as a Poiseuille flow:

$$\mathbf{u}(r) = V(r)\hat{\mathbf{x}}, \quad V(r) = \frac{2Q}{\pi a^4}(a^2 - r^2) \tag{6}$$

where $\mathbf{u}(r)$ is the flow velocity at r, $\hat{\mathbf{x}}$ is a unit vector along the cylinder, a is the radius of the cylinder and r is the distance from the centre of the cylinder and Q is the volumetric flow rate. The mean volumetric flow rate through the common carotid artery (CCA) has been measured as approximately 6 ml s^{-1} (Marshall et al., 2004), and the inner radius as 3 mm (Polak et al., 1996). Eq. (6) is used to estimate $\mathbf{u}$ at 6 μm; approximately the height of an endothelial cell. The shear rate k is found by comparing this solution with a simpler model for the flow, $\mathbf{u}(\mathbf{x}) = kz\hat{\mathbf{x}}$, simple shear flow, which we assume is a good approximation near the arterial wall. The viscosity of the fluid was taken to be 1cP.

A.2. GTPase model parameters

Parameters were found from (in order of preference) experimental data, from previous modelling work or were estimated.

For the force activation of Src, reaction (5), the parameters were estimated by comparison with an experimental time course (Jalali et al., 1998) for Src activation due to shear stress. The form of $k_+(z_e)$ was taken as $k_+(z_e) = k_+ + k_m/(1+e^{10-z_e})$. To estimate k_+, k_m and k_- the level of Src was assumed to be in a steady state S (in the absence of diffusion):

$$S = \frac{k_+ + \frac{k_m}{1+e^{10-z_e}}}{k_+ + \frac{k_m}{1+e^{10-z_e}} + k_-}$$

By integrating this function over a square (as an approximation to the cell) and assuming a linear relationship (in the downstream half of the cell) between z_e and the distance from the centre of the cell an expression for the fold increase in Src can be reached. Comparing this with the experimental observations (Jalali et al., 1998; Fleming et al., 2005) of a characteristic 2–5 fold increase in activated Src leads to a relationship between k_+, k_m and k_-. A second relationship can be drawn by comparing the order of activation of Src in the model with experimental data. Solving the ODE for reaction (5), gives a characteristic time for Src to be maximally activated; the solution has a $-D \cdot \exp(-(k_+ + k_m + k_-)t)$ term, so as $t \to \infty$ the activated Src level approaches its maximum. This maximum is observed within 4–10 min, hence $(k_+ + k_m + k_-)t$ must be large for t in this range. To finalise the parameter values a third relationship is assumed, following previous authors (Fußet al., 2007): initially the steady state level of activated Src is $\approx$ 1% of the total, so $100k_+ = k_-$. These relationships are sufficient to estimate $k_+ = 0.00006\ s^{-1}$, $k_- = 0.006\ s^{-1}$ and $k_m = 0.0147\ s^{-1}$.

The parameters for the Kelvin body, Fig. 5, were taken from previously reported modelling and experimental work (Mazzag et al., 2003; Bausch et al., 1999). Note that these parameters were derived by attaching a microbead to the cell surface, with an estimated area of approximately 6 μm^2 attached to the cell (Bausch et al., 1998). Hence, to correctly apply these parameters to the Kelvin body the f_i (note that this is a force per area, equation (2)) have to be scaled by 6 μm^2.

It was found that the GAP and GEF activation rates were not the rate limiting steps in network, Fig. 7. However, the rate-limiting step of conversion from the GDP- to GTP-bound form of Rac is dependent on GEF activity. Hence, provided the GEF activation rate was sufficiently fast then the rate-limiting Rac activation could be initiated early enough so that it occurred on a similar time scale to observed (Tzima et al., 2002). Hence, it was necessary to have the Rac GEF activating quickly, on the order of a minute. Similarly, the Rho GAP was also required to become activated quickly. These criterion determined the rates for the Rho GAP, and Rac GEF. Similar rates were taken for the corresponding Rac GAP and Rho GEF. However, they were altered slightly so that there were similar basal levels of the active form (otherwise the basal level of Src gives a bias to the Rho GAP and the Rac GEF). Rates were finally fixed by demanding a low ratio initially of active to inactive forms, and by (following the onset of flow) demanding the new level of active GAP or GEF was significantly less than the total (to avoid saturation). Initial total concentration of Rac and Rho (either active, inactive or bound in intermediary complexes) was taken to be 10 μM of each, which is a typical cellular amount (Jilkine et al., 2007; Goryachev and Pokhilko, 2006). Total concentration of RacGAP and RhoGAP, RhoGEF and RacGEF was taken to be 1, 1, 2, and 2 μM; with corresponding (initial) active concentrations 0.46, 0.75, 0.41 and 0.24 μM.

The parameters governing GTPase cycling between GTP and GDP bound states were found to be the most significant in governing the response; fortunately experimental data was available for this data (Goryachev and Pokhilko, 2006; Zhang et al., 1997, 2000).

References

Arthur, W., Petch, L., Burridge, K., 2000. Integrin engagement suppresses RhoA activity via a c-src dependent mechanism. Current Biology 10, 719–722.

Ballerman, B., Dardik, A., Eng, E., Liu, A., 1998. Shear stress and the endothelium. Kidney International 67 (54), 100–108.

Barbee, K.A., Davies, P.F., Lal, R., 1994. Shear stress-induced reorganization of the surface topography of living endothelial cells imaged by atomic force microscopy. Circulation Research 74 (1), 163–171.

Bausch, A., Möller, W., Sackmann, E., 1999. Measurement of local viscoelasticity and forces in living cells by magnetic tweezers. Biophysical Journal 76, 573–579.

Bausch, A., Ziemann, F., Boulbich, A., Jacobson, K., Sackmann, E., 1998. Local measurements of viscoelastic parameters of adherent cell surfaces by magnetic bead mircorheometry. Biophysical Journal 75, 2038–2049.

Bement, W., Miller, A., von Dassoq, G., 2006. Rho GTPase activity zones and transient contractile arrays. BioEsssays 28, 983–993.

Blake, J., 1971. A note on the image system for a stokeslet in a no-slip boundary. Proceedings of the Cambridge Philosophical Society 70, 303–310.

Bos, J., Rehmann, H., Wittinghofer, A., 2007. GEFs and GAPs: Critical elements in the control of small G proteins. Cell 129 (5), 865–877.

Chiu, Y.-J., Fujiwara, E., McBeath, K., 2008. Mechanotransduction in an extracted cell model: Fyn drives stretch- and flow-elicited pecam-1 phosphorylation. Journal of Cell Biology 182 (4), 753–763.

Civelekoglu-Scholey, G., Orr, A., Novak, I., Meister, J.-J., Schwartz, M., Mogilner, A., 2005. Model of coupled transient changes of Rac, Rho, adhesions and stress fibers alignment in endothelial cells responding to shear stress. Journal of Theoretical Biology 232, 569–585.

Davies, P., 1995. Flow-mediated endothelial mechanotransduction. Physiology Review 75, 519–569.

Davies, P., Robotewskyj, A., Griem, M., 1994. Quantitative studies of endothelial cell adhesion: directional remodelling of focal adhesion sites in response to flow forces. Journal of Clinical Investigation 93, 2031–2038.

DerMardirossian, C., Bokoch, G., 2005. GDIs: central regulatory molecules in rho GTPase activation. Trends in Cell Biology 15 (7), 356–363.

Ferko, M.C., Bhatnagar, A., Garcia, M.B., Butler, P.J., 2007. Finite-element stress analysis of a multicomponent model of sheared and focally-adhered endothelial cells. Annals of Biomedical Engineering 35 (2), 208–223 〈http://www.springerlink.com/content/1851534232118n2u/〉.

Fleming, I., Fisslthaler, B., Dixit, M., Busse, R., 2005. Role of PECAM-1 in the shear-stress-induced activation of akt and the endothelial nitric oxide synthase (enos) in endothelial cells. Journal of Cell Science 118 (18), 4103–4111.

Fuß, H., Dubitzky, W., Downes, C., Kurth, M., 2007. Deactivation of Src family kinases: Hypothesis testing using a monte carlo sensitivity analysis of systems-level properties. Journal of Computational Biology 14 (9), 1185–1200.

Garrett, T., Buul, J.V., Burridge, K., 2007. VEGF-induced Rac1 activation in endothelial cells is regulated by the guanine nucleotide exchange factor Vav2. Experimental Cell Research 313, 3285–3297.

Goldfinger, L., Tzima, E., Stockton, R., Kiosses, W.B., Kinbara, K., Tkachenko, E., Gutierrez, E., Groisman, A., Nguyen, P., Chien, S., Ginsberg, M.H., 2008. Localized 4 integrin phosphorylation directs shear stress–induced endothelial cell alignment. Circulation Research 103, 177–185.

Goryachev, A., Pokhilko, A., 2006. Computational model explains high activity and rapid cycling of Rho GTPases within protein complexes. PLoS Computational Biology 2 (12), e172.

Hazel, A., Pedley, T., 2000. Vascular endothelial cells minimize the total force on their nuclei. Biophysical Journal 78, 47–64.

Herant, M., Marganski, W.A., Dembo, M., 2003. The mechanics of neutrophils: synthetic modeling of three experiments. Biophysical Journal 84 (5), 3389–3413.

Higdon, J., 1985. Stokes flow in arbitrary two-dimensional domains: shear flow over ridges and cavities. Journal of Fluid Mechanics 159, 195–226.
Jaffe, A., Hall, A., 2005. Rho GTPases: biochemistry and biology. Annual Review in Cell Development Biology 21, 247–269.
Jalali, S., Li, Y.-S., Sotoudeh, M., Yuan, S., Li, S., Chien, S., Shyy, J.Y.-J., 1998. Shear stress activates p60src-Ras-MAPK signaling pathways in vascular endothelial cells. Arteriosclerosis, Thrombosis, and Vascular Biology 18, 227–234.
Jilkine, A., Marèe, A., Edelstein-Keshet, L., 2007. Mathematical model for spatial segregation of the Rho-family GTPases based on inhibitory crosstalk. Bulletin of Mathematical Biology 69 (6), 1943–1978.
Kawano, Y., Fukata, Y., Oshiro, N., Amaon, M., Nakamura, T., Ito, M., Matsumura, F., Inagaki, M., Kaiibuchi, K., 1999. Phosphorylation of myosin binding submit (mbs) of myosin phosphatase by Rho-kinase in vivo. Journal of Cell Biology 147, 1023–1037.
Marèe, A., Jilkine, A., Grieneisen, A.D.V., Edelstein-Keshet, L., 2006. Polarization and movement of keratocytes: a multiscale modelling approach. Bulletin of Mathematical Biology 68, 1169–1211.
Marshall, I., Papathanasopoulou, P., Wartolowska, K., 2004. Carotid flow rates and flow division at the bifurcation in healthy volunteers. Physiology Measurements 25, 691–697.
Martinac, B., 2004. Mechanosensitive ion channels: molecules of mechanotransduction. Journal of Cell Science 117, 2449–2460.
Mazzag, B., Tamaresis, J., Barakat, A., 2003. A model for shear stress sensing and transmission in vascular endothelial cells. Biophysical Journal 84, 4087–4101.
McCue, S., Danjnowiec, D., Xu, F., Zhang, M., Jackson, M., Languille, B.L., 2006. Shear stress regulates forward and reverse planar cell polarity of vascular endothelium in vivo and in vitro. Circulation Research 98, 939–946.
Narang, A., 2006. Spontaneous polarization in eukaryotic gradient sensing: A mathematical model based on mutual inhibition of frontness and backness pathways. Journal of Theoretical Biology 4 (21), 538–553.
Narumiya, S., Yasuda, S., 2006. Rho GTPases in animal cell mitosis. Current Opinion in Cell Biology 18 (2), 199–205.
Okud, M., Takahashi, M., Suero, J., Murry, C.E., Traub, O., Kawakatsu, H., Berk, B., 1999. Shear stress stimulation of p130cas tyrosine phosphorylationrequires calcium-dependent c-src activation. The Journal of Biological Chemistry 274 (28), 26803–26809.
Polak, J., Kronmal, R., Tell, G., O'Leary, D., Savage, P., Gardin, J., Rutan, G., Borhani, N., 1996. Compensatory increase in common carotid artery diameter. Stroke 27, 2012–2015.
Pozrikidis, C., 1992. Boundary Integral and Singularity Methods for Linearized Viscous Flow. Cambridge University Press.
Price, T., 1985. Slow linear shear flow past a hemispherical bump in a plane wall. Quarterly Journal of Mechanics and Applied Mathematics 38, 93–104.
Ridley, A., 2001. Rho GTPases and cell migration. Journal of Cell Science 114, 2713–2722.
Ridley, A., 2006. Rho GTPases and actin dynamics in membrane protrusions and vesicle trafficking. Trends in Cell Biology 16 (10), 552–559.
Riento, K., Ridley, A., 2003. ROCKs: multifunctional kinases in cell biology. Review in Molecular Cell Biology 4, 446–456.
Ross, R., 1999. Atherosclerosis — an inflammatory disease. Mechanism of Disease, The New England Journal of Medicine 340 (2), 115–126.
Rossman, K.L., Der, C.J., Sondek, J., 2005. Gef means go: turning on rho gtpases with guanine nucleotide-exchange factors. Nature Reviews Molecular Cell Biology 6 (2), 167–180 〈http://www.nature.com/nrm/journal/v6/n2/abs/nrm1587.html〉.
Saad, Y., 1981. Krylov subspace methods for solving large unsymmetric linear systems. Mathematics of Computation 37 (155), 105–126.
Sakumura, Y., Tsukada, Y., Yamamoto, N., Ishii, S., 2005. A molecular model for axon guidance based on cross talk between rho GTPases. Biophysical Journal 89 (2), 812–822.
Sawada, Y., Tamada, M., Dubin-Thaler, B.J., Cherniavskaya, O., Sakai, R., Tanaka, S., Sheetz, M., 2006. Force sensing by mechanical extension of the src family kinase substrate p130cas. Cell 127, 1015–1026.
Schwarz, U., Erdmann, T., Bischofs, I., 2005. Focal adhesions as mechanosensors: the two-spring model. Biosystems 83 (2–3), 225–232.
Stamenovic, D., Fredberg, J., ButlerWang, J.P., Ingber, D.E., 1996. A microstructural approach to cytoskeletal mechanics based on tensegrity. Journal of Theoretical Biology 181, 125–136.
Tcherkezian, J., Lamarche-Vane, N., 2007. Current knowledge of the large Rho GAP family of proteins. Biology Cell 99 (2), 67–86.
Tzima, E., del Pozo, M., Kiosses, W., Mohamed, S., Schwartz, M., 2002. Activation of Rac1 by shear stress in endothelial cells mediates both cytoskeletal reorganization and effects on gene expression. The EMBO Journal 21 (24), 6791–6800.
Tzima, E., del Pozo, M., Shattil, S.J., Chien, S., Schwartz, M., 2001. Activation of integrins in endothelial cells by fluid shear stress mediates Rho-dependent cytoskeletal alignment. EMBO Journal 20 (17), 4639–4647.
Tzima, E., Irani-Tehrani, M., Kiosses, W., Dejana, E., Schultz, D., Engelhardt, B., Cao, G., Delisser, H., Schwartz, M., 2005. A mechanosensory complex that mediates the endothelial cell response to fluid shear stress. Nature 437, 426–431.
Wang, Y., Botvinick, E., Zhao, Y., Berns, M.W., Usami, S., Tsien, R.Y., Chien, S., 2005a. Visualizing the mechanical activation of Src. Nature 434, 1040–1045.
Wang, Y., Botvinick, E.L., Zhao, Y., Berns, M.W., Usami, S., Tsien, R.Y., Chien, S., 2005b. Visualizing the mechanical activation of src. Nature 434 (7036), 1040–1045.
Wang, Y., Dimitrakopoulos, P., 2006a. Nature of the hemodynamic forces exerted on vascular endothelial cells or leukocytes adhering to the surface of blood vessels. Physics of Fluids 18 087107–1.
Wang, Y., Dimitrakopoulos, P., 2006b. Normal force exerted on vascular endothelial cells. Physical Review Letters 96 028106–1.
Wee, H., Oh, H.-M., Jo, J.-H., Jun, C.-D., 2009. Icam-1/lfa-1 interaction contributes to the induction of endothelial cell–cell separation: implication for enhanced leukocyte diapedesis. Experimental and Molecular Medicine 41 (5), 341–348.
Weinbaum, S., Tzeghai, G., Ganatos, P., Pfeffer, R., Chien, S., 1985. Effect of cell turnover and leaky junctions on arterial macromolecular transport. American Journal of Physiology 248, H945–H960.
Wojciak-Stothard, B., Ridley, A., 2003. Shear stress-induced endothelial cell polarization is mediated by Rho and Rac but not Cdc42 or PI 3-kinases. Journal of Cell Biology 161 (2), 429–439.
Zhang, B., Wang, Z.-X., Zheng, Y., 1997. Characterization of the interactions between the small GTPase Cdc42 and its GTPase-activating roteins and utative effectors. Journal of Biology and Chemistry 272 (35), 21999–22007.
Zhang, B., Zhang, Y., Wang, Z.-X., Zheng, Y., 2000. The role of cofactor in the guanine nucleotide exchange and GTP-hydrolysis reactions of Mg^{2+} rho family gtp-binding proteins. Journal of Biology and Chemistry 275 (33), 25299–25307.